# Theoretical Investigations on Oxidative Stability of Solvents and Oxidative Decomposition Mechanism of Ethylene Carbonate for Lithium Ion Battery Use

**ARTICLE** *in* THE JOURNAL OF PHYSICAL CHEMISTRY B · NOVEMBER 2009

Impact Factor: 3.3 · DOI: 10.1021/jp9074064 · Source: PubMed

# Theoretical Investigations on Oxidative Stability of Solvents and Oxidative Decomposition Mechanism of Ethylene Carbonate for Lithium Ion Battery Use

**Lidan Xing, Weishan Li,* Chaoyang Wang, Fenglong Gu, Mengqing Xu, Chunlin Tan, and Jin Yi**

*School of Chemistry and Environment and Key Lab of Electrochemical Technology on Energy Storage and Power Generation in Guangdong Universities, South China Normal University, Guangzhou 510006, China*

*Received: August 01, 2009; Revised Manuscript Received: September 25, 2009*

The electrochemical oxidative stability of solvent molecules used for lithium ion battery, ethylene carbonate (EC), propylene carbonate, dimethyl carbonate, diethyl carbonate, and ethyl methyl carbonate in the forms of simple molecule and coordination with anion $PF_6^-$, is compared by using density functional theory at the level of B3LYP/6-311++G (d, p) in gas phase. EC is found to be the most stable against oxidation in its simple molecule. However, due to its highest dielectric constant among all the solvent molecules, EC coordinates with $PF_6^-$ most strongly and reaches cathode most easily, resulting in its preferential oxidation on cathode. Detailed oxidative decomposition mechanism of EC is investigated using the same level. Radical cation $EC^{\bullet+}$ is generated after one electron oxidation reaction of EC and there are five possible pathways for the decomposition of $EC^{\bullet+}$ forming $CO_2$, CO, and various radical cations. The formation of CO is more difficult than $CO_2$ during the initial decomposition of $EC^{\bullet+}$ due to the high activation energy. The radical cations are reduced and terminated by gaining one electron from anode or solvent molecules, forming aldehyde and oligomers of alkyl carbonates including 2-methyl-1,3-dioxolane, 1,3,6-trioxocan-2-one, 1,4,6,9-tetraoxaspiro[4.4]nonane, and 1,4,6,8,11-pentaoxaspiro[4.6]undecan-7-one. The calculation in this paper gives a detailed explanation on the experimental findings that have been reported in literatures and clarifies the mechanism on the oxidative decomposition of EC.

## 1. Introduction

Lithium ion battery has found its wider and wider application in various fields such as electronic devices, tools, and vehicles, because it provides high energy density, three times more than conventional lead acid or nickel-hydride batteries.[1−6] However, its safety needs to be improved, especially as the power sources for electric vehicles.[7] Many factors can cause the safety problem of lithium ion battery but the key point is the electrolyte using organic molecules as solvents, which may decompose under any abuse of battery. Solvents used for the electrolyte are composed mainly of linear alkyl carbonates, such as dimethyl carbonate (DMC), diethyl carbonate (DEC), and ethyl methyl carbonate (EMC), and cyclic alkyl carbonates, such as ethylene carbonate (EC) and propylene carbonate (PC). The former have low viscosity and the latter have high dielectric permittivity; the combination of both carbonates provides the electrolyte with high ionic conductivity. Unlike PC, which can be cointercalated into graphite anode with lithium ions, EC is not cointercalated into graphite but helps to build an effective solid electrolyte interphase (SEI) that can inhibit the decomposition of solvent molecules on the anode.[8,9] Therefore, EC is ubiquitous and an indispensable component of electrolytes for lithium ion battery.

The chemical stability of the solvents affects not only the safety but also capacity density and cyclic stability of lithium ion battery. To improve the performance of lithium ion battery, it is necessary to understand the decomposition mechanism of solvents in electrolytes. The decomposition of solvents usually takes place on anode or cathode. The reductive decomposition of solvents on the anode can be inhibited to a great extent by using SEI forming additives, such as vinylene carbonate (VC),[10,11] ethylene sulfite (ES),[12,13] and propane sultone (PS).[14] On the other hand, the oxidative decomposition of solvents happens more easily on cathode when the battery is overcharged. Several methods have been proposed to prevent the battery from overcharge, including external protection device and internal additives such as redox shuttles and polymerizable compounds.[15,16] However, these protection methods are not perfect. The safety that an external protection device provides depends on the reliability of the electronic device. The redox shuttles are not appropriate because of their low diffusion coefficients. The polymerizable compounds are shutdown additives. Therefore, the oxidative decomposition of solvents should be avoided to keep the battery safe, which needs the understanding of the oxidative decomposition mechanism.

Much experimental work has been focused on the oxidative decomposition of solvents on cathodes of lithium ion battery,[17−23] but the oxidative decomposition mechanisms of solvents were less understood. Recently, a detailed mechanism on the oxidative decomposition of PC was given with theoretical calculations,[24] which can explain all of the experimental phenomena that have been reported in literatures. As an essential component of solvents for lithium ion battery, however, the oxidative decomposition mechanism of EC has not yet been understood and some controversial explanations to the experimental results can be found in literatures. For example, epoxy ethane is a controversial intermediate. Arakawa et al. proposed that the oxidative mechanism of EC involving epoxy ethane as an intermediate.[19] Moshkovich et al. gave a different explanation, which did not involve epoxy ethane.[20]

In this work, the oxidative stability of the solvent molecules, including EC, PC, DMC, DEC, and EMC, in the forms of simple molecule and coordination with anion $PF_6^-$ was compared and the detailed oxidative decomposition mechanism of EC was

* To whom correspondence should be addressed. Tel.: +86 20 39310256. Fax: +86 20 39310256. E-mail: liwsh@scnu.edu.cn.

10.1021/jp9074064 
Published on Web 11/30/2009

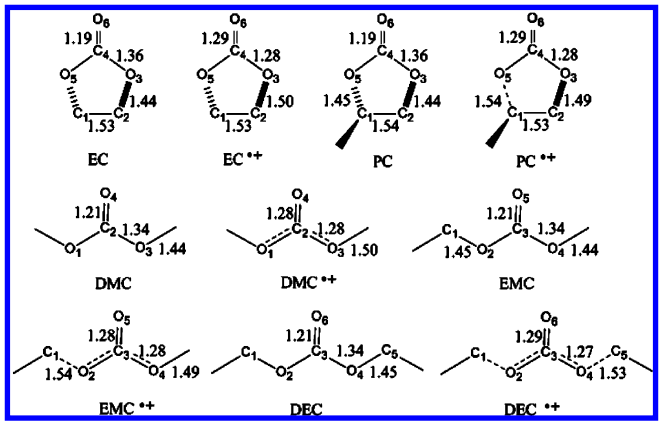


**Figure 1.** Geometry of solvents optimized from B3LYP/6-311++G (d,p).

**TABLE 1: The Thermodynamic Properties (in kJ/mol) and Frontier Molecular Orbital Energy (in eV) of Various Solvents in Gas Phase**

| | EC | PC | EMC | DMC | DEC |
|---|---|---|---|---|---|
| $\Delta E_{AIE}$ | 1024.24 | 1002.93 | 987.91 | 1004.55 | 972.24 |
| $\Delta E_{VIE}$ | 1092.46 | 1062.45 | 1032.45 | 1055.88 | 1011.88 |
| $\Delta H$ | 1022.62 | 1000.34 | 982.87 | 1000.00 | 966.92 |
| $\Delta G$ | 1019.75 | 997.71 | 974.04 | 993.38 | 958.09 |
| HOMO | −8.46 | −8.37 | −8.11 | −8.21 | −8.05 |
| LUMO | −0.60 | −0.62 | −0.25 | −0.23 | −0.26 |

given based on the calculation using density functional theory (DFT) at the level of B3LYP/6-311++G (d, p).

## 2. Computational Methods

All the calculations were performed using the Gaussian 03 package.[25] The equilibrium and transition state structures were optimized by B3LYP[26] method in conjunction with the 6-311++G(d,p) basis set.[27] To confirm each optimized stationary point and make zero-point energy (ZPE) corrections, frequency analyses were done with the same basis set. To confirm transition state (TS) connected with corresponding products (or intermediates) and reactants (or intermediates), intrinsic reaction coordinate (IRC) calculation was also performed at the same level. Enthalpy and Gibbs free energy were obtained at 298.2 K. The charge distribution was analyzed by the natural bond orbital (NBO) theory.

## 3. Results and Discussion

**3.1. Oxidative Stability of Solvents.** The optimized geometry and the selected structural parameter of EC, PC, DMC, DEC, EMC, and their radical cations are presented in Figure 1. After losing an electron, PC, EMC, and DEC experience the breaking of $C_1-O_5$, $C_1-O_2$, $C_1-O_2$, and $O_4-C_5$, respectively (as shown in Figure 1 by single-dotted line), while the geometry of EC and DMC does not show significant change.

**TABLE 2: The Binding Energy (in kJ/mol) of Solvent Molecules with $PF_6^-$ in Gas Phase**

| | EC + $F_6P^-$ | PC + $F_6P^-$ | EMC + $F_6P^-$ | DMC + $F_6P^-$ | DEC + $F_6P^-$ |
|---|---|---|---|---|---|
| $\Delta E$ | −64.51 | −63.96 | −22.83 | −23.59 | −21.86 |
| $\Delta E + \Delta ZPE$ | −61.99 | −61.58 | −21.69 | −22.94 | −21.86 |
| $\Delta H$ | −58.63 | −60.70 | −17.92 | −18.89 | −19.42 |
| $\Delta G$ | −32.40 | −24.38 | 2.87 | −1.45 | 10.62 |

Table 1 lists the frontier molecular orbital energy and the thermodynamic properties for the solvent oxidation in gas phase. In Table 1, the adiabatic ionization energy $E_{AIE} = E_c - E_n$ and vertical ionization energy $E_{VIE} = E_n^+ - E_n$. $E_n$ is the neutral geometry energy, $E_n^+$ is cation energy with optimized neutral geometry, and $E_c$ is the energy with cation geometry. On the basis of the molecular orbital theory, the ability of one molecule to lose or gain electron depends on the energy level of the highest occupied molecular orbital (HOMO) or the lowest unoccupied molecular orbital (LUMO). The HOMO energy of EC, PC, DMC, DEC, and EMC is −8.46, −8.37, −8.21, −8.05, and 8.11 eV, respectively, indicating that the oxidative decomposition activity is in the order DEC > EMC > DMC > PC > EC. The same conclusion can be drawn from the thermodynamic data in Table 1. This result is consistent with the report in the reference.[21]

On the basis of the calculations above, it seems that EC is the most stable against oxidation among all the solvent molecules. However, due to the higher dielectric constant of cyclic alkyl carbonates than linear alkyl carbonates, the anion of the electrolyte salt, for example, $PF_6^-$ in $LiPF_6$, is coordinated more easily with cyclic alkyl carbonates than linear alkyl carbonates. The interaction strength between the solvent and $PF_6^-$ can be quantified by calculating the binding energy of the formation of the ion−solvent complex, which has been defined as the difference between product and reactant energy. The geometry of the complexes of EC, PC, DMC, DEC, and EMC with $PF_6^-$ is optimized and shown in Figure 2. Table 2 lists the binding energy corresponding to the several complexes in gas phase. It should be noted from Table 2 that the interactions between $PF_6^-$ anion and cyclic carbonates are stronger, especially the interaction with EC, than those between $PF_6^-$ and linear alkyl carbonates. The negative charge tends to transfer

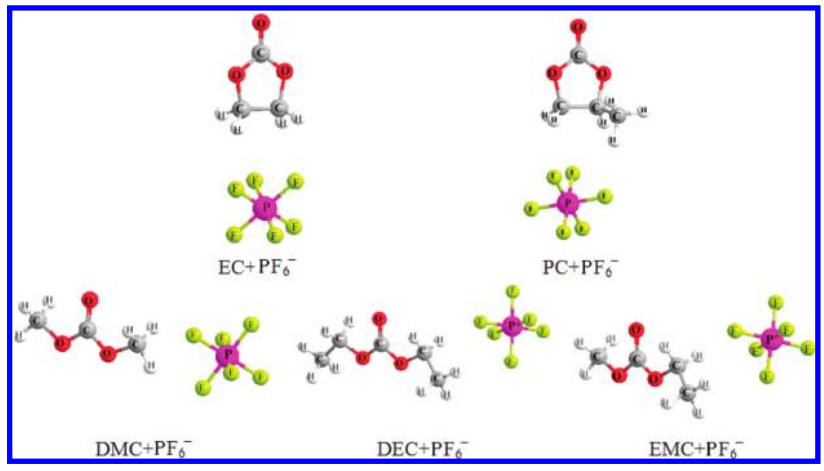


**Figure 2.** Geometry of the complexes of EC, PC, DMC, DEC, and EMC with $PF_6^-$ optimized from B3LYP/6-311++G (d,p).

**TABLE 3: Atomic Charge of EC and $EC^{\bullet+}$ in Gas Phase Based on NPA**

| atom | $C_1$ | $C_2$ | $O_3$ | $C_4$ | $O_5$ | $O_6$ |
|---|---|---|---|---|---|---|
| EC | −0.05 | −0.05 | −0.55 | 1.01 | −0.55 | −0.56 |
| $EC^{\bullet+}$ | −0.06 | −0.06 | −0.41 | 0.99 | −0.41 | −0.01 |

to cathode when the battery is charged. Thus, $EC-PF_6^-$ reaches cathode more easily than other solvent molecules, resulting in its preferential oxidation on cathode when lithium ion battery is charged. This calculation is in agreement with experimental results. For example, Joho et al. reported that EC was preferentially oxidized in an electrolyte using EC/DMC as solvent.[28] Moshkovich et al. also showed that EC was more reactive than the other alkyl carbonates in electrochemical oxidation reactions.[20]

**3.2. Oxidative Decomposition Mechanism of EC.** ***3.2.1. Initial Oxidation of EC.*** The initial oxidation of EC involves a one-electron transfer from EC molecule to cathode, resulting in radical cation ($EC^{\bullet+}$). The optimized geometry and the selected structural parameter of $EC^{\bullet+}$ are presented in Figure 1. The charge distribution on atoms in EC and $EC^{\bullet+}$ obtained by natural population analysis (NPA) in gas phase is listed in Table 3. Charge is mainly observed on C and O atoms in EC and $EC^{\bullet+}$. It can be found that before and after EC loses one electron, the charge on C atoms is almost the same, while the charge on O atoms changes in various magnitudes. The charge change on $O_6$ atom is from −0.56 to −0.01 and the change on $O_3$ and $O_5$ is from −0.55 to −0.41. This indicates that the electron is bereaved from O atoms during the initial oxidation of EC, especially from $O_6$ atom.

On the basis of the geometry of $EC^{\bullet+}$, it can be known that there are five possible pathways for its decomposition, involving five initial products (EC-1, EC-2, EC-3, EC-4, and EC-5), four intermediates (M1, M2, M3, and M4), and nine transition states (TS1, TS2, TS3, TS4, TS5, TS6, TS7, TS8, and TS9), as shown in Scheme 1.

The geometry of all the relative intermediates, transition states and initial products involved in Scheme 1 is presented in Figure 3. The potential energy ($\Delta E + \Delta ZPE$) profile of oxidative decomposition for $EC^{\bullet+}$ is shown in Figure 4. The calculated relative energy ($\Delta E$ in kJ/mol), enthalpy ($\Delta H$ in kJ/mol), and free energy ($\Delta G$ in kJ/mol) of the stationary points are listed in Table 4. To confirm the geometry of transition states, frequency analyses and IRC calculations are carried out and the calculated imaginary frequency ($\omega$ in $cm^{-1}$) of the transition states for the oxidative decomposition of $EC^{\bullet+}$ is included in Table 4. Each transition state (TS1, TS2, TS3, TS4, TS5, TS6, TS7, TS8, and TS9) corresponds to one imaginary frequency (464, 553, 426, 688, 415, 437, 124, 235, and 569 $i$ $cm^{-1}$), and each transition state has been confirmed by IRC calculation, indicating that all the transition states are connected with the relevant reactants and products.

A ring-opening reaction of $EC^{\bullet+}$ has been detected both by Matsushita et al.[29] and Joho et al.[28] using in situ FTIR on electrochemical oxidation of EC. Ring-opening of $EC^{\bullet+}$ could happen via TS1 and TS3 as shown in Scheme 1, leading to radical cations M1 and M2, respectively. The energy barrier of the former is roughly four times higher than that of the later (161.5 and 40.1 kJ/mol for TS1 and TS3, respectively). This indicates that M2 forms more easily than M1. EC-1 is formed via the transition state TS2 from M1 with the direct cleavage of $C_4-O_5$ bond (path 1) and the corresponding activation energy is 36.7 kJ/mol. There are four possible pathways for M2 to dissociate. Two pathways release gas product $CO_2$ via TS4 (path 2) and TS7 (path 4). The other two pathways release gas product CO via transition states TS5 and TS6 (path 3) and via transition states TS8 and TS9 (path 5). In path 2, M2 converts into EC-2 via TS4, with the direct cleavage of $C_2-O_3$ bond, the corresponding activation energy is 65.2 kJ/mol, 9.0 kJ/mol higher than that of the conversion of M2 to EC-4 via TS7 in path 4. In path 3, M2 converts into cation M3 via TS5, with a direct cleavage of $C_1-H_8$ bond, corresponding to activation energy

**SCHEME 1: Possible Pathways for the Decomposition of $EC^{\bullet+}$**

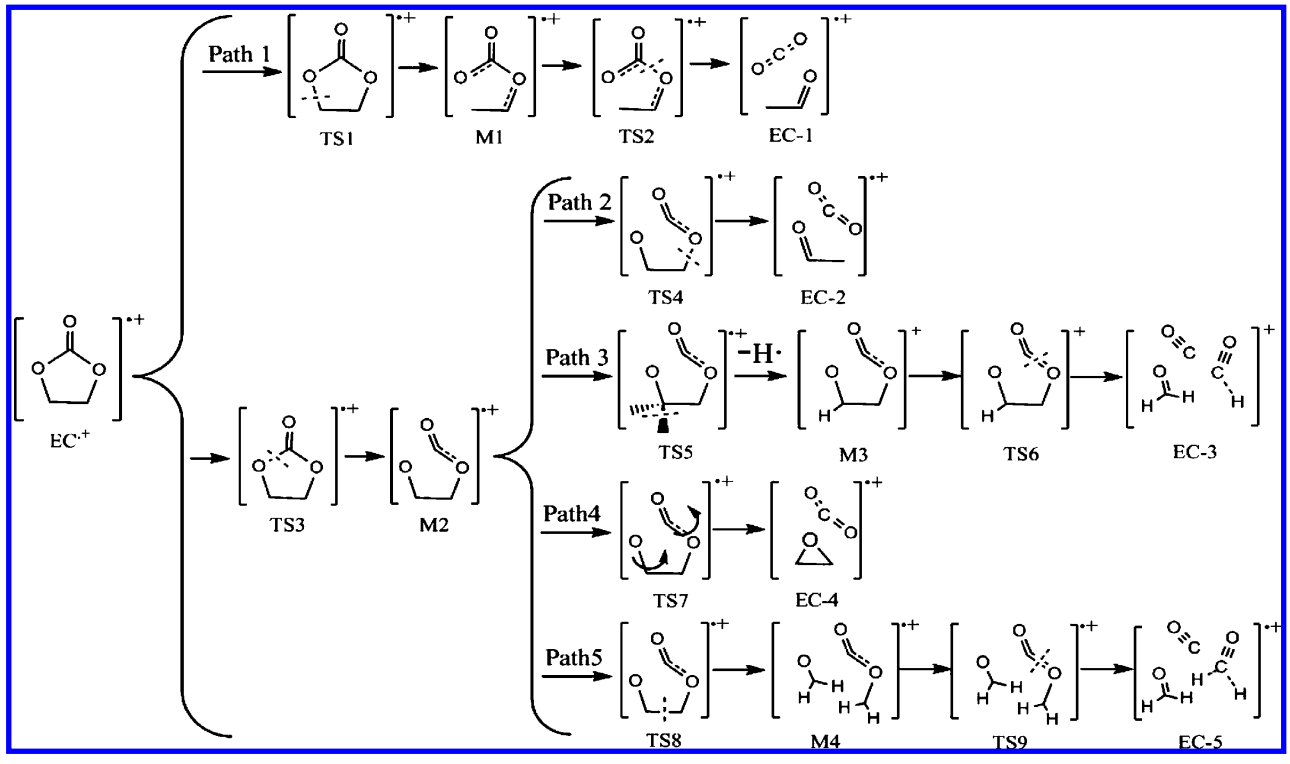

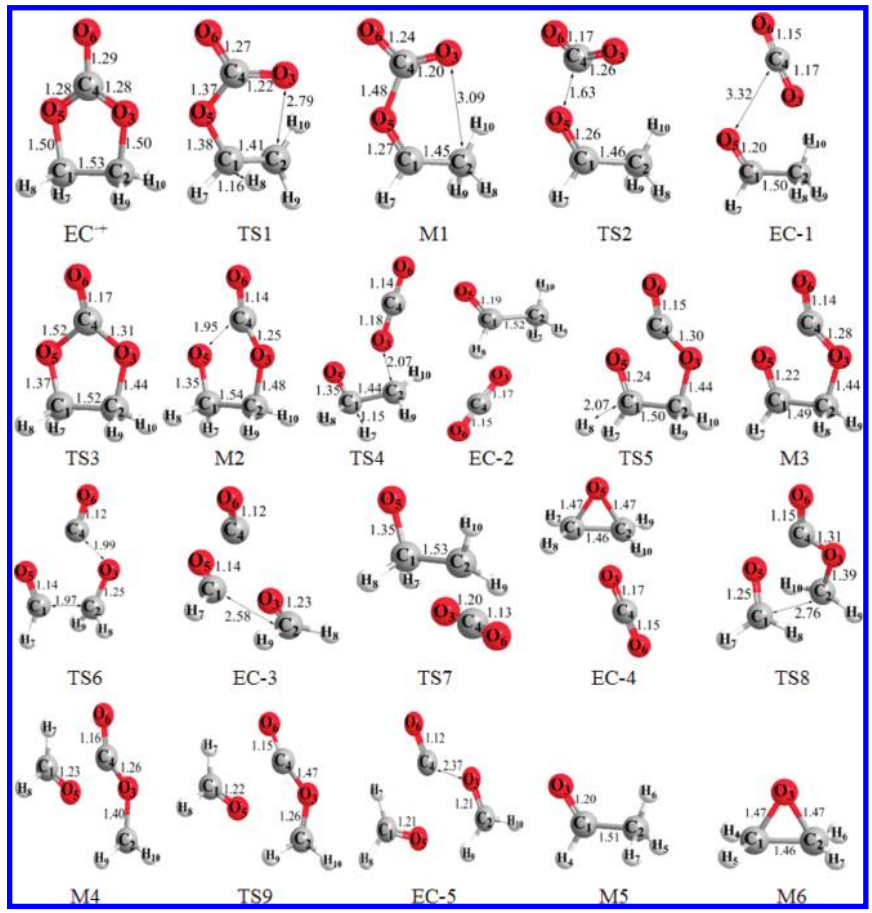


**Figure 3.** The optimized geometry of the various reactants, intermediates, transition states, and initial oxidative products of EC•+, at B3LYP/6-311++G (d,p) level. Bond lengths are in angstrom.

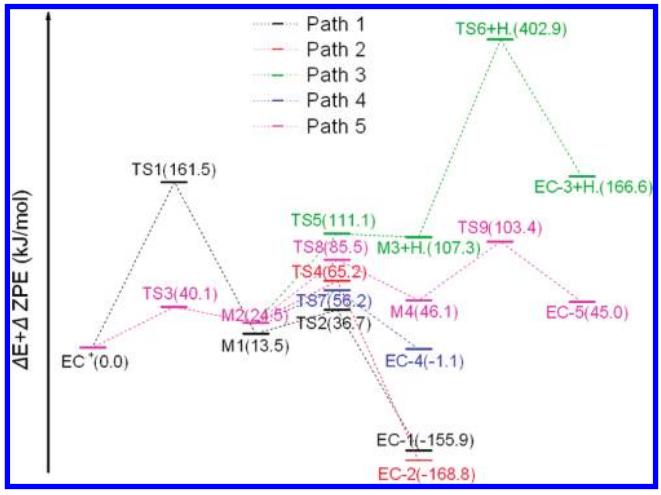


**Figure 4.** Potential energy profile for the decomposition process of EC•+, calculated with B3LYP/6-311++ (d, p).

of 111.1 kJ/mol. Subsequently, M3 could dissociate to EC-3 via TS6, with a higher energy barrier than the other transition states (402.9 kJ/mol for TS6 + H•, H• is released from M2 via TS5). In path 5, M2 converts into radical cation M4 via TS8 with a direct cleavage of $C_1-C_2$ bond, corresponding to activation energy of 85.5 kJ/mol. M4 could dissociate to EC-5 via TS9 with a direct cleavage of $C_3-O_4$ bond and the corresponding activation energy is 103.4 kJ/mol.

On the basis of the discussion above, it can be found that path 4 would be the most probable reaction for the decomposition of EC•+, followed by path 2, path 5, path 3, and path 1.

**TABLE 4: Relative Energy, Enthalpy, and Free Energy (in kJ/mol) of the Stationary Points, and Imaginary Frequency ($\omega$/cm$^{-1}$) of the Transition States for the Oxidative Decomposition of EC•+**

| structure | $\Delta E$ | $\Delta E + \Delta$ZPE | $\Delta H$ | $\Delta G$ | $\omega$ |
|---|---|---|---|---|---|
| EC•+ | 0.0 | 0.0 | 0.0 | 0.0 | |
| TS1 | 166.0 | 161.5 | 163.7 | 158.7 | 464 *i* |
| M1 | 31.1 | 13.5 | 17.7 | 6.8 | |
| TS2 | 40.8 | 36.7 | 40.8 | 29.4 | 553 *i* |
| EC-1 | −134.6 | −155.9 | −147.8 | −171.8 | |
| TS3 | 41.8 | 40.1 | 40.2 | 39.8 | 426 *i* |
| M2 | 35.1 | 24.5 | 27.0 | 20.9 | |
| TS4 | 73.5 | 65.2 | 70.1 | 54.6 | 688 *i* |
| EC-2 | −145.8 | −168.8 | −160.6 | −186.4 | |
| TS5 | 140.2 | 111.1 | 113.0 | 110.2 | 415 *i* |
| M3+H• | 140.8 | 107.3 | 113.8 | 81.8 | |
| TS6+H• | 457.2 | 402.9 | 414.0 | 370.6 | 437 *i* |
| EC-3+H• | 219.9 | 166.6 | 182.9 | 120.4 | |
| TS7 | 40.9 | 56.2 | 41.4 | 42.8 | 124 *i* |
| EC-4 | 19.0 | −1.1 | 6.4 | −18.7 | |
| TS8 | 103.7 | 85.5 | 88.5 | 82.8 | 235 *i* |
| M4 | 67.1 | 46.1 | 53.4 | 37.0 | |
| TS9 | 128.2 | 103.4 | 110.1 | 94.4 | 569 *i* |
| EC-5 | 78.4 | 45.0 | 58.4 | 20.0 | |

This implies that $CO_2$ is the most possible product through path 4, and the formation of CO is more difficult than $CO_2$ during the decomposition of EC•+. The data of $\Delta E$, $\Delta H$, and $\Delta G$ show the same results. Therefore, the content of the initial products should be in the order as M2 > EC-4> EC-2 > EC-5 > M3 > EC-1 > EC-3 ≈ M1.

The products EC-5, M3, EC-1, EC-3, and M1 can be ignored due to the high activation energy. The residual radical cation

**TABLE 5: Atomic Charge of TS5, M2, M3, M5, M6, EC-1, EC-2, EC-3, EC-4, and EC-5 Based on NPA**

| | TS5 | M2 | M3 | M5 | M6 | EC-1 | EC-2 | EC-3 | EC-4 | EC-5 |
|---|---|---|---|---|---|---|---|---|---|---|
| $C_1$ | 0.38 | −0.15 | 0.48 | 0.46 | −0.07 | 0.46 | 0.46 | 0.68 | −0.07 | 0.33 |
| $C_2$ | −0.12 | −0.03 | −0.13 | −0.62 | −0.07 | −0.64 | −0.62 | 0.41 | −0.07 | 0.34 |
| $O_3$ | −0.46 | −0.44 | −0.44 | 0.00 | 0.04 | −0.54 | −0.58 | −0.43 | −0.58 | −0.29 |
| $C_4$ | 1.02 | 1.04 | 1.03 | | | 1.02 | 1.04 | 0.41 | 1.02 | 0.60 |
| $O_5$ | −0.40 | −0.20 | −0.40 | | | −0.05 | −0.06 | −0.28 | 0.03 | −0.34 |
| $O_6$ | −0.36 | −0.31 | −0.33 | | | −0.39 | −0.40 | −0.40 | −0.41 | −0.42 |
| $H_8$ | 0.14 | 0.31 | | | | 0.29 | 0.32 | | 0.27 | 0.19 |

structures of EC-2 and EC-4 after the emission of $CO_2$ are indexed as M5 and M6, respectively, which are also presented in Figure 3. For M2, the bond length of $C_1-O_5$ is 1.35 Å, which is distinctly longer than the standard bond length of C═O (1.22 Å) in aldehyde and close to the standard single-bond length of C−O (1.36 Å) in ester. This indicates that $C_1-O_5$ in M2 prefers to form a single bond. For M5, the bond length of $C_1-O_3$ is 1.20 Å, which is close to the standard double-bond length of C═O in aldehyde. This indicates that $C_1-O_3$ in M5 trends to form double bond. For M6, $O_3$ is connected with $C_1$ and $C_2$ to form a planar three-member ring, with the bond length of $C_1-O_3$ (or $C_2-O_3$) being 1.47 Å, which is close to that of the single-bond length of C−O (1.43 Å) in alcohols. This indicates that $C_1-O_3$ (or $C_2-O_3$) should be a single bond. Therefore, radical termination reaction is much easier for M2 than M5 and M6.

***3.2.2. Charge Distribution of the Relative Products.*** Table 5 presents the charge on atoms in TS5, M2, M3, M5, M6, EC-1, EC-2, EC-3, EC-4, and EC-5. The sum of the charge on $O_3$, $C_4$, and $O_6$ of $CO_2$ in EC-1, EC-2, and EC-4 is 0.09, 0.06, and 0.03, respectively. The charge on $C_4$ and $O_6$ of CO in EC-3 and EC-5 is 0.01 and 0.18, respectively. All the charge on the atoms in $CO_2$ and CO is small, indicating that, after the decomposition of $EC^{\bullet+}$, $CO_2$, and CO maintain electrical neutrality and the positive charge mainly concentrates on the residual structure in EC-1, EC-2, EC-3, EC-4, and EC-5. To determine whether the hydrogen released from TS5 is cation or radical, the atomic charges on atoms of M2 and TS5 are calculated and the results are also presented in Table 5. It can be seen from Table 5 that after the cleavage of $C_1-H_8$ bond, charge on $H_8$ in M2 and TS5 is 0.31 to 0.14, respectively. This indicates that with the cleavage of $C_1-H_8$ bond the electron is transferred to $H_8$, forming radical $H^{\bullet}$ and cation M3.

To determine the termination reaction activity of the radical cation, M2, M5 and M6, the charges on the atoms of these radical cations are calculated. The atomic charges located on $O_5$ in M2, and $O_3$ in M5 and M6 are −0.20, 0.00 and 0.04, respectively, as shown in Table 5. The charge density on $O_5$ in M2 is higher than those on $O_3$ in M5 and M6. This result, combing the bonding situation of $O_5$ in M2 and $O_3$ in M5 and M6, shows that M2 is more active than M5 and M6 for the radical termination. M5 and M6 will prefer to be reduced rather than radical termination.

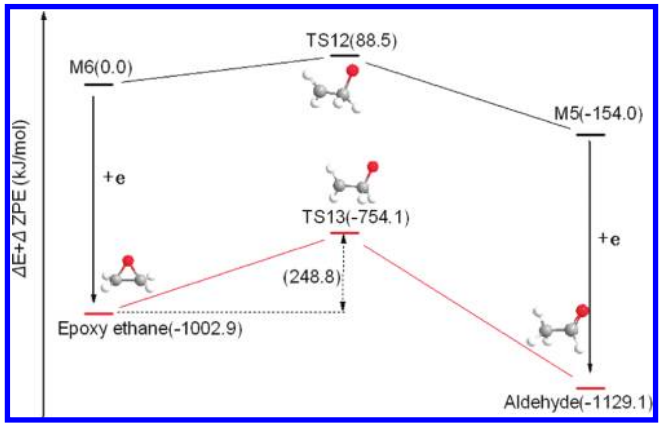


**Figure 5.** Potential energy profile for the termination reaction of M5 and M6 by reduction, calculated with B3LYP/6-311++ (d, p).

**TABLE 6: Relative Energies, Enthalpies, and Free Energies (in kJ/mol) of the Stationary Points, and Imaginary Frequency ($\omega$/cm$^{-1}$) of the Transition States for the Termination Reaction of M5 and M6**

| structure | $\Delta E$ | $\Delta E + \Delta$ZPE | $\Delta H$ | $\Delta G$ | $\omega$ |
|---|---|---|---|---|---|
| M5 | −150.8 | −154.0 | −152.5 | −156.1 | |
| M6 | 0.0 | 0.0 | 0.0 | 0.0 | |
| TS12 | 95.9 | 88.5 | 88.3 | 87.9 | −414i |
| aldehyde | −1132.4 | −1129.1 | −1128.1 | −1000.7 | |
| epoxy ethane | −1011.2 | −1002.9 | −1003.8 | −1000.7 | |
| TS13 | −744.6 | −754.1 | −753.9 | −753.3 | −678i |

**3.3. Termination Reaction of M5 and M6.** The potential energy ($\Delta E + \Delta$ZPE) profile for the termination reaction of M5 and M6 through reduction is presented in Figure 5, and the specific data are listed in Table 6. As shown in Figure 5, M6 could convert into a more stable radical cation M5 via transition state TS12 with activation energy of 88.5 kJ/mol, or gain one electron to form epoxy ethane, with formation heat of −1002.9 kJ/mol. Epoxy ethane may isomerize to form a more stability product aldehyde, via transition state TS13, the corresponding activation energy is 248.8 kJ/mol. Aldehyde also can be formed through one electron reduction of M5 with formation heat of −975.1 kJ/mol. Therefore, aldehyde should be the main reduction product of M5 and M6.

**3.4. Termination Reaction of M2.** Figure 6 presents the possible termination reaction processes of M2. There are three possible transition states, TS (2-4), TS (6-9) and TS (7-8). Specific data for all the stationary points are presented in Table 7. M2 terminates through direct reduction (gain one electron on anode or from solvent) forming (1) EC with exothermic energy of 1046.6 kJ/mol. Nucleophilicly attacking the carbonyl carbon of another M2, M2 could undergo dimerization probably without barrier (the transition state cannot be found) forming (11), which has two positive charges, and (11) could undergo further reduction by gaining two electrons and releasing $CO_2$ and $H_2$ forming oligomer (13) 1,3-dioxolane-2,4-dione and ethylene with exothermic energy of 1077.9 kJ/mol. Considering M2 is surrounded by more EC than M2, the possibility of dimerization reaction is minor. Thus $H_2$ is not the oxidative decomposition product of EC. The radical center of M2 could attack the carbonyl carbon of EC without barrier forming (2). (2) may terminate through reduction forming oligomer (3) 1,4,6,8,11-pentaoxaspiro[4.6]undecan-7-one with exothermic energy of 999.4 kJ/mol or by releasing $CO_2$ via TS (2-4) (the energy barrier is 35.0 kJ/mol) forming (4). (4) has one positive charge and could undergo further reduction forming oligomer (5) 1,4,6,9-tetraoxaspiro[4.4]nonane, with exothermic energy 1046.7 kJ/mol. One of the possible products, $C_6H_8O_6$, from the

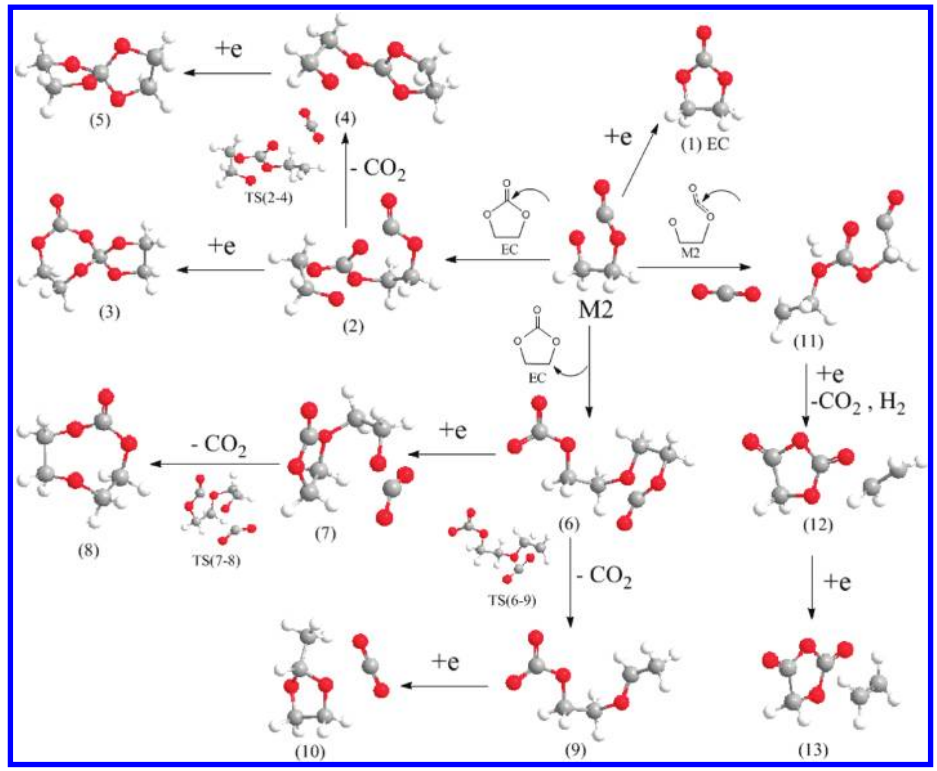


**Figure 6.** Possible termination ways of radical cation M2.

**TABLE 7: Relative Energies, Enthalpies, and Free Energies (in kJ/mol) of the Stationary Points, and Imaginary Frequency ($\omega$/cm$^{-1}$) of the Transition States for the Termination Reaction of M2**

| structure | $\Delta E$ | $\Delta E$ + ZPE | $\Delta H$ | $\Delta G$ | $\omega$ |
|---|---|---|---|---|---|
| M2 | 0.0 | 0.0 | 0.0 | 0.0 | |
| 1 | −1059.3 | −1046.6 | −1049.6 | −1040.7 | |
| 2/2 | −569.0 | −558.2 | −560.1 | −529.5 | |
| 3/2 | −1015.6 | −999.4 | −1003.6 | −966.6 | |
| TS(2-4) | −551.5 | −548.7 | −549.1 | −523.7 | −94i |
| (4 + $CO_2$)/2 | −639.2 | −630.3 | −631.4 | −622.8 | |
| (5 + $CO_2$)/2 | −1058.3 | −1046.7 | −1049.1 | −1037.0 | |
| 6/2 | −565.8 | −554.4 | −555.9 | −527.8 | |
| 7/2 | −947.1 | −934.0 | −936.6 | −902.6 | |
| TS(7-8)/2 | −942.4 | −931.1 | −933.7 | −900.0 | −208i |
| (8 + $CO_2$)/2 | −1072.7 | −1061.0 | −1063.2 | −1050.0 | |
| TS(6-9)/2 | −548.7 | −545.3 | −545.3 | −523.7 | −123i |
| (9 + $CO_2$)/2 | −636.4 | −632.8 | −632.0 | −629.0 | |
| (10 + $CO_2$)/2 | −1128.8 | −1122.8 | −1121.4 | −1121.9 | |
| 11/2 | −46.8 | −49.5 | −46.9 | −27.7 | |
| (12 + $CO_2$ + $H_2$)/2 | −605.5 | −618.4 | −614.1 | −628.1 | |
| (13 + $CO_2$ + $H_2$)/2 | −1048.6 | −1063.0 | −1057.2 | −1077.9 | |

oxidative decomposition of EC, was reported to have the same molecular weight with (3), but the authors ascribed it as a chain molecule.[20]

The radical center of M2 may attack the alkyl carbon of EC without barrier forming (6). (6) may terminate through reduction to form (7) with exothermic energy of 934.0 kJ/mol, or release $CO_2$ via TS (6−9) (the energy barrier is 34.4 kJ/mol) forming (9), (9) has one positive charge and could undergo further reduction forming oligomer (10) 2-methyl-1,3-dioxolane and $CO_2$ with exothermic energy of 1122.8 kJ/mol. This termination should be the most probable reaction, because its Gibbs free energy ($\Delta G$ = −1121.9 kJ/mol) is the most negative among all the involved reactions for the oxidative decomposition of EC. (7) could terminate by releasing $CO_2$ via TS (7−8) (the energy barrier is 9.4 kJ/mol) forming oligomer (8) 1,3,6-trioxocan-2-one with exothermic energy of 1061.0 kJ/mol. Both (8) and (10) has the C−O−C−O−C skeletal vibration. Joho et al. detected C−O−C−O−C skeletal vibration in the system of 1 M $LiPF_6$ in EC.[28] This may be the proof for the existence of the products (10) and (8).

On the basis of the results above, the most favorable thermodynamically oligomer of alkyl carbonate from the oxidative decomposition of EC is 2-methyl-1,3-dioxolane, followed by 1,3,6-trioxocan-2-one, 1,4,6,9-tetraoxaspiro[4.4]nonane and 1,4,6,8,11-pentaoxaspiro [4.6] undecan-7-one.

## 4. Conclusions

Compared with the solvent molecules, propylene carbonate, dimethyl carbonate, diethyl carbonate, and ethyl methyl carbonate, used for electrolytes of lithium ion battery, ethylene carbonate coordinates more strongly with anion $PF_6^-$ in lithium salt and thus tends to be oxidized preferably on cathode of the battery. Radical cation $EC^{\bullet+}$ is generated after EC transfers one electron to cathode, and there are five possible pathways for the decomposition of $EC^{\bullet+}$ forming $CO_2$, CO, and various radical cations. The formation of CO is more difficult than $CO_2$ during the initial decomposition of $EC^{\bullet+}$ due to the high activation energy. The radical cations are reduced and terminated by gaining one electron from anode or solvent molecules, forming aldehyde and oligomers of alkyl carbonates. The most favorable thermodynamically oligomer of alkyl carbonate from the oxidative decomposition of EC is 2-methyl-1,3-dioxolane, followed by 1,3,6-trioxocan-2-one, 1,4,6,9-tetraoxaspiro[4.4]nonane and 1,4,6,8,11-pentaoxaspiro[4.6]undecan-7-one.

**Acknowledgment.** This work is supported by the National Natural Science Foundation of China (NNSFC, No. 20873046), Specialized Research Fund for the Doctoral Program of Higher Education (No. 200805740004) and Key project of Guangdong Province (No. 2009B050700039).

## References and Notes

(1) Wang, Q.; Evans, N.; Zakeeruddin, S. M.; Exnar, I.; Grätzel, M. *J. Am. Chem. Soc.* **2007**, *129*, 3163.

(2) Xu, K. *Chem. Rev.* **2004**, *104*, 4303.

(3) Tarascon, J. M.; Armand, M. *Nature* **2001**, *414*, 359.

(4) Armstrong Robert, A.; Tee, D. W.; Mantia, F. L.; Novăk, P.; Bruce, P. G. *J. Am. Chem. Soc.* **2008**, *130*, 3554.

(5) Tasaki, K. *J. Phys. Chem. B* **2005**, *109*, 2920.

(6) Aurbach, D.; Levi, M. D.; Levi, E.; Schechter, A. *J. Phys. Chem. B* **1997**, *101*, 2195.

(7) Wang, L.; Maxisch, T.; Ceder, G. *Chem. Mater.* **2007**, *19*, 543.

(8) Zhang, H. L.; Sun, C. H.; Li, F.; Liu, C.; Tan, J. H.; Cheng, M. *J. Phys. Chem. C* **2007**, *111*, 4740.

(9) Xing, L. D.; Wang, C. Y.; Xu, M. Q.; Li, W. S.; Cai, Z. P. *J. Power Sources* **2009**, *189*, 689.

(10) Wang, Y. X.; Nakamura, S.; Tasaki, K.; Balbuena, P. B. *J. Am. Chem. Soc.* **2002**, *124*, 4408.

(11) Aurbach, D.; Gamolsky, K.; Markovsky, B.; Gofer, Y.; Schmidt, M.; Heider, U. *Electrochim. Acta* **2003**, *47*, 1423.

(12) Wrodnigg, G. H.; Besenhard, J. O.; Winter, M. *J. Electrochem. Soc.* **1999**, *146*, 470.

(13) Ota, H.; Sato, T.; Suzuki, H.; Usami, T. *J. Power Sources* **2001**, *97*−*98*, 107.

(14) Xu, M. Q.; Li, W. S.; Lucht, B. L. *J. Power Sources* **2009**, *193*, 804.

(15) Xu, M. Q.; Xing, L. D.; Li, W. S.; Zuo, X. X. *J. Power Sources* **2008**, *184*, 427.

(16) Zhang, S. S. *J. Power Sources* **2006**, *162*, 1394.

(17) Matsuta, S.; Kato, Y.; Ota, T.; Kurokawa, H.; Yoshimura, S.; Fujitani, S. *J. Electrochem. Soc.* **2001**, *148*, A7.

(18) Ufheil, J.; Wursig, A.; Schneider, O. D.; Novak, P. *Electrochem. Commun.* **2005**, *7*, 1380.

(19) Arakawa, M.; Yamaki, J. *J. Power Sources* **1995**, *54*, 250.

(20) Moshkovich, M.; Cojocaru, M.; Gottlieb, H. E.; Aurbach, D. *J. Electroanal. Chem.* **2001**, *497*, 84.

(21) Zhang, X. R.; Pugh, J. K.; Ross, P. N. *J. Electrochem. Soc.* **2001**, *148*, E183.

(22) Xu, K.; Angell, C. A. *J. Electrochem. Soc.* **1998**, *145*, L70.

(23) Xu, K.; Ding, S.; Jow, T. R. *J. Electrochem. Soc.* **1999**, *146*, 4172.

(24) Xing, L. D.; Wang, C. Y.; Li, W. S.; Xu, M. Q.; Meng, X. L.; Zhao, S. F. *J. Phy. Chem. B* **2009**, *113*, 5181.

(25) Frisch, M. J.; Trucks, G. W.; Schlegel, H. B.; Scuseria, G. E.; Robb, M. A.; Cheeseman, J. R.; Montgomery, J. A.; Vreven, Jr. T.; Kudin, K. N.; Burant, J. C.; Millam, J. M.; Iyengar, S. S.; Tomasi, J.; Barone, V.; Mennucci, B.; Cossi, M.; Scalmani, G.; Rega, N.; Petersson, G. A.; Nakatsuji, H.; Hada, M.; Ehara, M.; Toyota, K.; Fukuda, R.; Hasegawa, J.; Ishida, M.; Nakajima, T.; Honda, Y.; Kitao, O.; Nakai, H.; Klene, M.; Li, X.; Knox, J. E.; Hratchian, H. P.; Cross, J. B.; Bakken, V.; Adamo, C.; Jaramillo, J.; Gomperts, R,; Stratmann, R. E.; Yazyev, O.; Austin, A. J.; Cammi, R.; Pomelli, C.; Ochterski, J. W.; Ayala, P. Y.; Morokuma, K.; Voth, G. A.; Salvador, P.; Dannenberg, J. J.; Zakrzewski, V. G.; Dapprich, S.; Daniels, A. D.; Strain, M. C.; Farkas, O.; Malick, D. K.; Rabuck, A. D.; Raghavachari, K.; Foresman, J. B.; Ortiz, J. V.; Cui, Q.; Baboul, A. G.; Clifford, S.; Cioslowski, J.; Stefanov, B. B.; Liu, G.; Liashenko, A.; Piskorz, P.; Komaromi, I.; Martin, R. L.; Fox, D. J.; Keith, T.; Al-Laham, M. A.; Peng, C. Y.; Nanayakkara, A.; Challacombe, M.; Gill, PM W.; Johnson, B.; Chen, W.; Wong, M. W.; Gonzalez, C.; Pople, J.A. *Gaussian 03*, Reversion B.05;Gaussian Inc.: Pittsburgh, PA, 2003.

(26) Abbotto, A.; Streitwieser, A.; Schleyer, P. R. *J. Am. Chem. Soc.* **1997**, *119*, 11255.

(27) Wang, Y.; Balbuena, P. B. *J. Phys. Chem. A* **2001**, *105*, 9972.

(28) Joho, F.; Novăk, P. *Electrochim. Aata* **2000**, *45*, 3589.

(29) Matsushita, T.; Dokko, K.; Kanamura, K. *J. Power Sources* **2005**, *146*, 360.

JP9074064